European Journal of Medicinal Chemistry 44 (2009) 4509–4515

Contents lists available at ScienceDirect

European Journal of Medicinal Chemistry

journal homepage: http://www.elsevier.com/locate/ejmech

Original article

Synthesis and characterization of the Zn(II) and Cu(II) piperidinyl isoeuxanthone complexes: DNA-binding and cytotoxic activity

Hui-Fang Wang [a], Rui Shen [b], Ning Tang [a,*]

[a] College of Chemistry and Chemical Engineering, State Key Laboratory of Applied Organic Chemistry, Lanzhou University, South Tianshui Road No. 222, Lanzhou 730000, PR China
[b] College of Pharmacy Nankai University, Tianjin 300071, PR China

ARTICLE INFO

Article history:
Received 20 July 2008
Received in revised form
14 June 2009
Accepted 15 June 2009
Available online 24 June 2009

Keywords:
1-Hydroxy-6-(2-(1-piperidinyl)ethoxy)xanthone
Zn(II) complex
Cu(II) complex
DNA-binding
Intercalative mode
Cytotoxic activity

ABSTRACT

Two new complexes $ZnL_2 \cdot 2H_2O$ (**1**) and $CuL_2 \cdot 2H_2O$ (**2**) (HL = 1-hydroxy-6-(2-(1-piperidinyl)ethoxy)xanthone) have been synthesized and characterized. Their interactions with calf thymus DNA (ct DNA) were investigated by absorption spectroscopy, fluorescence spectroscopy, ethidium bromide (EB) displacement experiments, circular dichroism spectroscopy and viscosity measurements. Experimental results suggested that there were intercalative interactions of the complexes with DNA. The binding affinity of complex **2** was higher than that of **1**. In addition, the cytotoxic effects of both complexes were evaluated with lung adenocarcinoma (GLC-82), esophagus squamous cancer (ECA109) and human gastric cancer (SGC7901) cells using MTT assay. Both were potent exhibiting significant cytotoxicity in vitro.

1. Introduction

Recently, increasing attention has been paid to xanthones that are widely present as a class of secondary metabolites in some higher plants and microorganisms [1–3]. These naturally occurring compounds and their synthetic analogs have demonstrated multiple pharmacological properties, such as anti-oxidant, anti-inflammatory, anti-malarial and anti-cancer activities, etc. [4–9]. Xanthones may be viewed as flavone derivatives having three linear aromatic rings in which the phenyl group is fused with two aromatic rings, as shown in Fig. 1(a). The structural similarity and biological efficacy of xanthones encouraged many scientists to isolate or synthesize appropriately modified derivatives for the development of prospective new drug candidates [10–13].

Several experiments have demonstrated that DNA is one of the intracellular targets of anti-cancer drugs that following their interactions with DNA will inhibit division of cancerous cell, cause DNA damage and result in cell death [14,15]. Previous studies have reported that two or more phenolic hydroxyl groups are fundamental structural elements underlying the inhibitory activity of these compounds via a mechanism that is so far unclear [16]. Therefore to enhance the activity of these compounds, structural modification of the phenolic hydroxyl group with different substituents is currently attempted [17–19].

Up to date, only few systematic studies have reported the interactions of xanthones and their derivatives with DNA, with a structure–activity relationship that remains to be established. Furthermore, the studies of the interactions of xanthone derivatives with diverse metal ions have been initiated in an attempt to examine the binding modes and possible synergetic effects. In this context introducing a piperidinyl group at position 6 of the isoeuxanthone may enhance the activity. We hereby describe in this paper the synthesis and identification of the mononuclear Zn(II) complex and Cu(II) complex with 1-hydroxy-6-(2-(1-piperidinyl)ethoxy)xanthone. We also have investigated the interactions of these complexes with calf thymus DNA using absorption spectroscopy, fluorescence spectroscopy, ethidium bromide (EB) displacement experiments, circular dichroism spectroscopy and viscosity measurements. In addition we have evaluated their cytotoxic effects against lung adenocarcinoma (GLC-82), esophagus squamous cancer (ECA109) and human gastric cancer (SGC7901) cells by MTT assay.

* Corresponding author. Tel.: +86 931 8911218; fax: +86 931 8912582.
E-mail address: tangn@lzu.edu.cn (N. Tang).

0223-5234/$ – see front matter © 2009 Elsevier Masson SAS. All rights reserved.
doi:10.1016/j.ejmech.2009.06.019

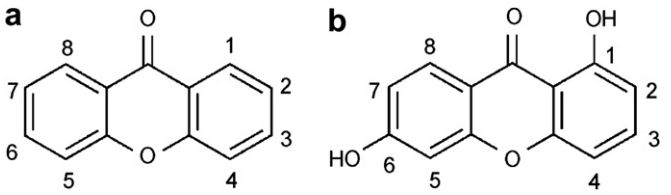

Fig. 1. (a) The structure of xanthone. (b) The structure of isoeuxanthone.

2. Results and discussion

2.1. Characterization of the complexes

2.1.1. Compositions and properties of the complexes

The results of elemental analyses, molar conductance, IR data, ^{1}H NMR and UV–vis measurements suggest that the compositions of the two metal complexes are $ZnL_2\cdot 2H_2O$ (**1**) and $CuL_2\cdot 2H_2O$ (**2**), where HL is 1-hydroxy-6-(2-(1-piperidinyl)ethoxy)xanthone (1-OH group deprotonated) and acts as a bidentate ligand binding to Zn(II) ion and Cu(II) ion, respectively. The proposed structures of the complexes are shown in Fig. 2. Both complexes are stable for extended periods in air, soluble in DMF, DMSO, slightly soluble in Me_2CO, $CHCl_3$, CH_3OH and CH_3CH_2OH, but insoluble in benzene. The molar conductance values suggest that both are non-electrolytes [20].

2.1.2. IR spectra

In the IR spectrum of the ligand [16], valance carbonyl group vibrations ν(C=O) coupled with the double band in the γ-benzopyrone ring appears at 1647 cm^{-1}. The absorption bands situated at 1608, 1574 and 1448 cm^{-1} are related to carbon vibration in benzene and γ-pyrone rings. However, the bands of ν(C=O) in **1** and **2** shift to 1616 and 1609 cm^{-1}, $\Delta\nu$ (ligand − complex) are to 31 and 38 cm^{-1}, respectively. These shifts demonstrate that the group loses its original characteristics and forms a coordinative bond with Zn(II) ion or Cu(II) ion. Due to the influence of the coordination, the bands assigned to γ-pyrone rings in complex **1** exhibit at 1566 and 1455 cm^{-1} while that in complex **2** exhibit at 1564 and 1458 cm^{-1}. The bands observed at 3418 and 523 cm^{-1} are attributed to ν(O–H) and ρ_w(O–H) of the coordinated water. The weak bands at 487 cm^{-1} and 484 cm^{-1} are assigned to ν(M–O) [21].

2.1.3. ^{1}H NMR spectra

^{1}H NMR spectra of **1** was studied using DMSO-d_6 as solvent. Compared the ^{1}H NMR of **1** with the ligand, the single peak (δ 12.75 ppm) assigned to the hydroxy proton (1-OH) of the free ligand disappeared [16]. The change indicates that the oxygen of the deprotonated hydroxy group in the ligand coordinates to Zn(II) ion. In addition, the shifts of the hydrogen in the phenyl were changed as a result of coordination.

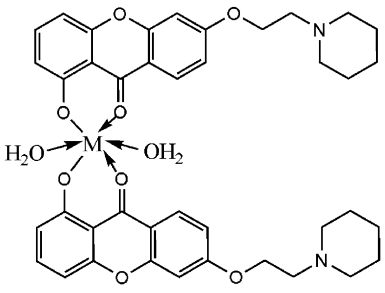

Fig. 2. The speculated structure of the complexes (M = Zn(II) ion, Cu(II) ion).

2.1.4. UV spectra

The studies of electronic spectra for the complexes and the ligand were carried out in CH_3CH_2OH. The electronic spectra of the ligand show a strong band at 227 nm, a medium band at 298 nm and a weak band at 353 nm. There are three bands at 229, 302 and 356 nm for the two complexes. These changes indicate that the complexes are formed.

2.1.5. Stoichiometry studies

To establish the stoichiometry between Zn(II) ion and the ligand in aqueous solution, continuous variation method was carried out by UV–vis spectroscopy [22]. Whereas the total mole concentration of Zn(II) ion and the ligand (L) was held constant ($C_{Zn} + C_L = 1.0 \times 10^{-5}$ M), the mole fraction of Zn(II) ion varied from 0.0 to 1.0. Fig. 3(a) shows a plot of absorption intensity variation with $C_{Zn}/(C_{Zn} + C_L)$, a maximal absorbance was obtained at a $C_{Zn}/(C_{Zn} + C_L)$ ratio of 1:3. Evidently, the stoichiometric composition of Zn(II) ion and the ligand is 1:2 under the conditions [23]. Similarly, the

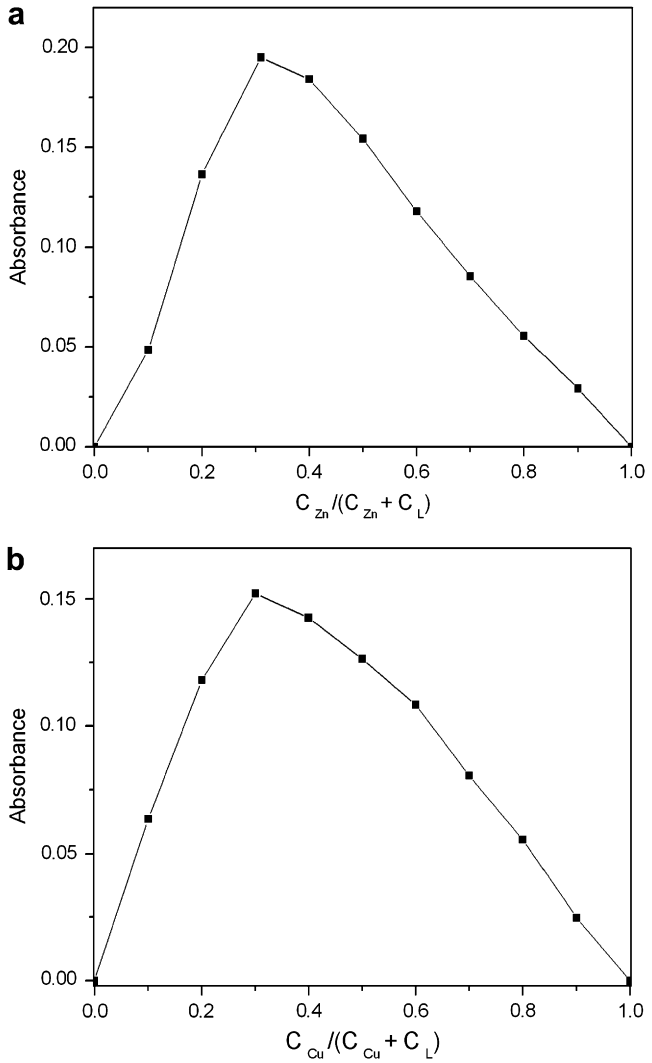

Fig. 3. (a) Plot of the complex formation of Zn(II) ion with ligand (L), monitored with a UV–vis spectrophotometer. (b) Plot of the complex formation of Cu(II) ion with ligand (L), monitored with a UV–vis spectrophotometer.

stoichiometric ratio of Cu(II) ion and the ligand in complex **2** was determined (Fig. 3(b)).

2.2. DNA-binding mode and affinity

2.2.1. Absorption spectra

Electronic absorption spectroscopy is universally employed to examine the binding mode of DNA with metal complexes [24,25]. The absorption spectra of **1** and **2** in the absence and presence of ct DNA are given in Fig. 4(a) and (b). In the absence of DNA, the absorption spectra of **1** has a strong π–π^* transition band at 229 nm, a medium n–π^* transition band at 302 nm and a weak n–π^* transition band at 356 nm. Complex **2** has similar absorption peaks to complex **1**. Increasing DNA concentration, the absorption bands of the two complexes show hypochromisms as well as slight red shift. These phenomena indicate that the complexes probably interact with ct DNA by intercalation mode, involving strong π-stacking interactions between xanthone rings of the complexes and DNA base pairs.

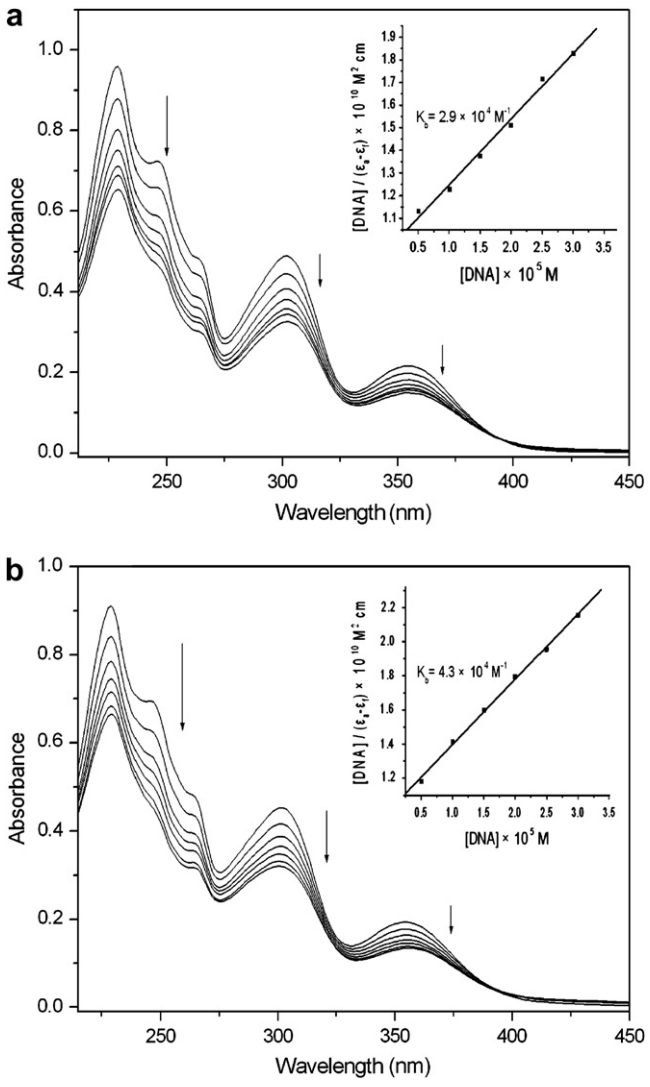

Fig. 4. (a) UV–vis absorption spectra of complex **1** (10 μM) in the presence of increasing amounts of ct DNA; [DNA] = 0, 5, 10, 15, 20, 25, 30 μM. The arrow indicates the absorbance change upon increasing DNA concentration. The inset is plot of [DNA]/($\varepsilon_b - \varepsilon_f$) vs [DNA] for the titration of DNA to complex **1**. (b) UV–vis absorption spectra of complex **2** (10 μM) in the presence of increasing amounts of ct DNA; [DNA] = 0, 5, 10, 15, 20, 25, 30 μM. The arrow indicates the absorbance changes upon increasing DNA concentration. The inset is a plot of [DNA]/($\varepsilon_b - \varepsilon_f$) vs [DNA] for the titration of DNA to complex **2**.

In order to study the binding ability of the compounds with DNA quantitatively, the binding constant K_b was determined by Eq. (1) [26],

$$[\mathrm{DNA}]/(\varepsilon_a - \varepsilon_f) = [\mathrm{DNA}]/(\varepsilon_b - \varepsilon_f) + 1/K_b(\varepsilon_b - \varepsilon_f) \quad (1)$$

where [DNA] is the concentration of DNA in base pairs, ε_a, ε_f, and ε_b are the apparent extinction coefficient corresponding to A_{obsd}/[M], the extinction coefficient for the free compound and the extinction coefficient for the compound in the fully bound form, respectively. In the plots of [DNA]/($\varepsilon_a - \varepsilon_f$) vs [DNA], K_b is given by the ratio of slope to the intercept (Fig. 4, inset). The binding constants K_b for **1** and **2** were found to be $2.9 \times 10^4\ M^{-1}$ and $4.3 \times 10^4\ M^{-1}$, respectively. The results indicate that the binding strength of **2** with DNA is stronger than that of **1**.

2.2.2. Fluorescence spectra

The binding mode of DNA with the two complexes was also investigated using fluorescence spectroscopy. Fixed amounts (10 μM) of the complexes were titrated with increasing amounts of ct DNA. Emission spectra for **1** and **2** are shown in Fig. 5(a) and (b). Enhanced fluorescence intensity was obtained with increasing DNA concentration indicating a deep intercalation of the complexes with DNA. The results are in agreement with other intercalators [27], suggesting efficient protection of the two complexes from water by the hydrophobic environment inside the DNA helix. This will restrict the mobility of the complexes at the binding site and decrease their vibrational modes of relaxation.

2.2.3. DNA–EB displacements

We further investigated the intercalation mode of the complexes binding to DNA using the competitive binding displacement experiment. EB is a conjugate planar molecule. Its fluorescence intensity is very weak, but it increases greatly when EB intercalates into the base pairs of double-stranded. When a second ligand which could compete with EB for DNA-binding sites was added, EB is free from DNA and the fluorescence quenching of DNA–EB system is observed. Therefore EB can be used as a common fluorescent probe for DNA structure and has been employed to investigate the mode and the process of metal complex binding to DNA [28,29]. The emission spectra of DNA–EB system upon the increasing amounts of **1** and **2** are shown in Fig. 6(a) and (b), respectively. The emission intensity of DNA–EB system at 587 nm decreased apparently when the concentration of the complexes increased and an isoactinic point appeared at about 544 nm. The phenomena suggest that the complexes can compete for DNA-binding sites with EB and displace EB from the DNA–EB system [30], which is usually characteristic of the intercalative interaction of compounds with DNA [31].

Interaction mode of compound binding to DNA can be determined according to the classical Stern–Volmer equation (2) [32,33]:

$$F_0/F = 1 + K_q[\mathrm{Q}] \quad (2)$$

where F_0 and F represent the emission intensity in the absence and presence of quencher, respectively, K_q is a linear Stern–Volmer quenching constant and [Q] is the quencher concentration. The quenching plots illustrate that the quenching of EB bound to DNA by the complexes is in good agreement with the linear Stern–Volmer equation (Fig. 6(a) and (b), inset). In the plots of F_0/F vs [Q], K_q is given by the ratio of the slope to the intercept. The K_q value for complex **1** is $2.4 \times 10^4\ M^{-1}$ while that for complex **2** is $4.0 \times 10^4\ M^{-1}$, which reveals that complex **2** has higher ability of replacing EB from DNA–EB system and stronger binding affinity to

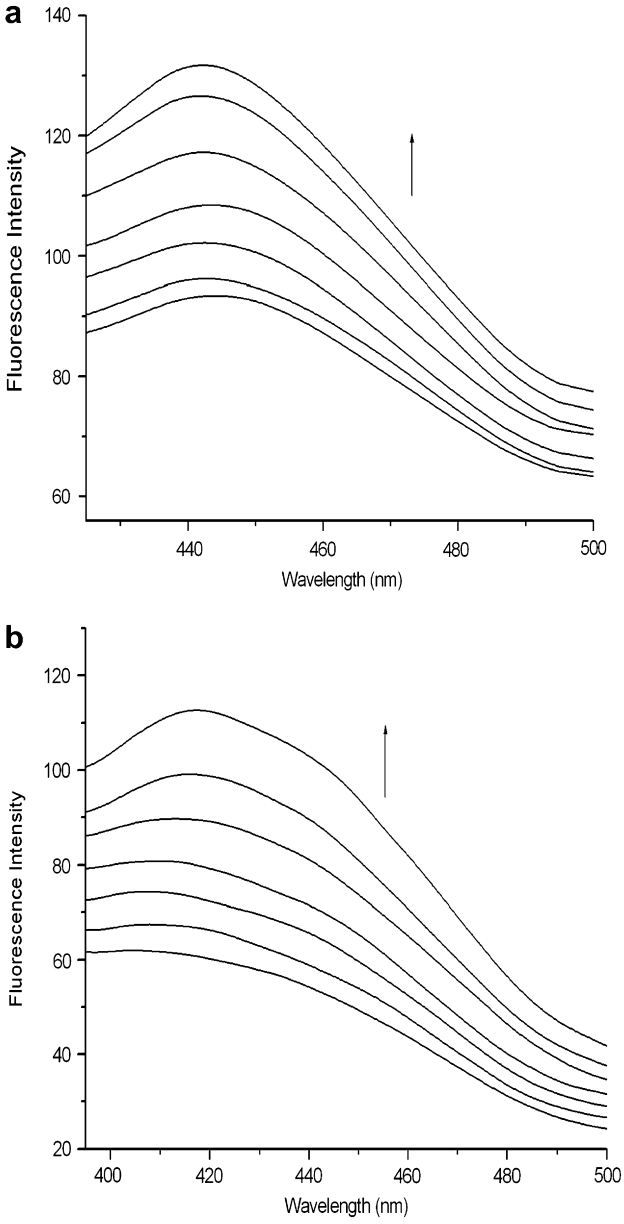

Fig. 5. (a) Fluorescence emission spectra of complex **1** (10 μM) in the presence of increasing amounts of ct DNA. (λ_{ex} = 346 nm, λ_{em} = 420–500 nm) [DNA] = 0, 2.5, 5, 7.5, 10, 12.5, 15 μM. The arrow indicates the emission intensity changes upon increasing DNA concentration. (b) Fluorescence emission spectra of complex **2** (10 μM) in the presence of increasing amounts of ct DNA. (λ_{ex} = 323 nm, λ_{em} = 420–500 nm) [DNA] = 0, 2.5, 5, 7.5, 10, 12.5, 15 μM. The arrow indicates the emission intensity changes upon increasing DNA concentration.

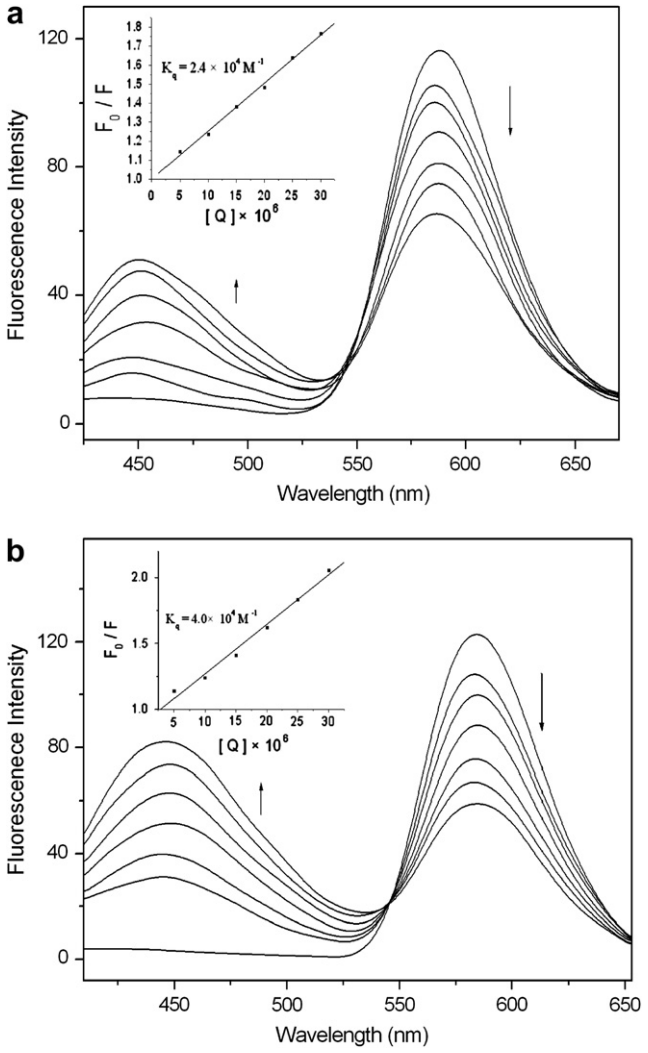

Fig. 6. (a) Fluorescence emission spectra of DNA–EB in the presence of 0, 5, 10, 15, 20, 25, 30 μM of **1**. (λ_{ex} = 346 nm, λ_{em} = 420–660 nm) [EB] = 2 μM, [DNA] = 30 μM. The inset is Stern–Volmer quenching plots of the fluorescence titration, $K_q = 2.4 \times 10^4\ M^{-1}$. (b) Fluorescence emission spectra of DNA–EB in the presence of 0, 5, 10, 15, 20, 25, 30 μM of **2**. (λ_{ex} = 346 nm, λ_{em} = 420–660 nm) [EB] = 2 μM, [DNA] = 30 μM. The inset is Stern–Volmer quenching plots of the fluorescence titration, $K_q = 4.0 \times 10^4\ M^{-1}$.

DNA than complex **1**. The result is in consistent with the binding constants determined by electronic absorption spectroscopy.

2.2.4. Circular dichroic spectral studies

Circular dichroic spectral techniques may give us useful information on how the conformation of the DNA chain is influenced by the bound complex. The CD spectrum of ct DNA consists of a positive band at 275 nm due to base-stacking and a negative band at 245 nm due to helicity, which is also characteristic of DNA in a right-handed B form [34]. The changes in CD signals of DNA observed on interaction with drugs may often be assigned to the corresponding changes in ct DNA structure [35]. Thus simple groove binding and electrostatic interaction of DNA with small molecules show less or no perturbation on the base-stacking and helicity bands, while intercalation enhances the intensities of both the bands and stabilizes the right-handed B conformation of ct DNA [36].

The CD spectra of ct DNA were monitored in the presence of **1** and **2**, respectively. As shown in Fig. 7, on addition of **1** to ct DNA, the CD spectra show intensity increase in the positive band and intensity decrease in the negative band with slight red shifts. While addition of **2** to ct DNA, the CD spectra shows more evident changes both in molar ellipticity and red shifts than **1** to ct DNA. These observations are supportive of the intercalative modes of DNA-binding to the complexes as reflected by the enhancement in the positive bands, and the partial unwinding of DNA helix as reflected by the intensity decrease in the negative bands [37,38]. These are similar to those observed for $[Ru(NH_3)_4(qdppz)]^{2+}$ [39] and $[Co(NH_3)_6]^{3+}$ bound to DNA of short lengths with 160 base pairs [40].

2.2.5. Viscosity measurements

Optical photophysical probes generally provide necessary, but not sufficient clues to support binding mode. Hydrodynamic measurements that are sensitive to length change (i.e., viscosity and sedimentation) are regarded as the least ambiguous and the most

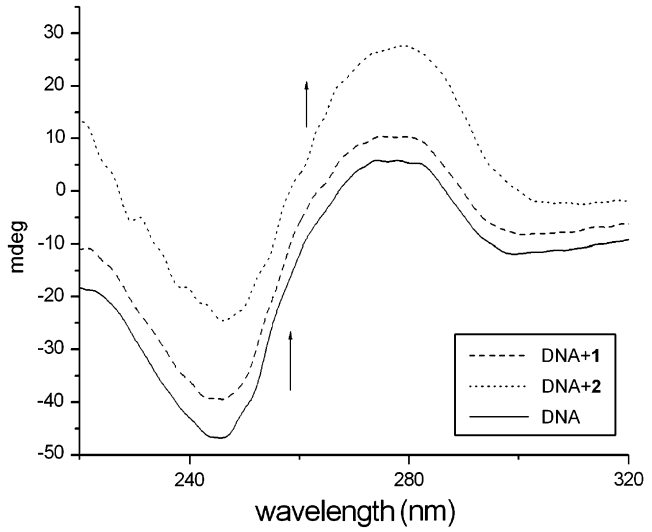

Fig. 7. CD Spectra of ct DNA (120 μM) in the absence and presence of **1** (40 μM) and **2** (40 μM).

critical tests of binding in solution in the absence of crystallographic structural data. A classical intercalation model results in lengthening the DNA helix as base pairs are separated to accommodate the binding small molecules, leading to an increase of DNA viscosity. In contrast, a partial and non-classical intercalation of small molecules could bend or kink the DNA helix, reduce its effective length and, concomitantly, its viscosity [27,41].

As a validation of the above verdict, viscosity measurements were carried out. The effects of the two complexes on the viscosity of DNA at 25.0 °C are shown in Fig. 8. It can be observed that the viscosity of the DNA increases steadily with increasing amounts of **1** or **2**. Such behavior is accordance with other intercalators, which increases the relative specific viscosity for the lengthening of the DNA double helix resulting from intercalation. These results indicate that the two complexes can intercalate the adjacent DNA base pairs, causing an extension in the helix, and thus increase the viscosity of DNA. As shown in Fig. 8, complex **2** can intercalate more deeply than complex **1**. The results obtained from viscosity studies also validate those obtained from the spectroscopic studies. On the basis of all the spectroscopic studies together with the viscosity

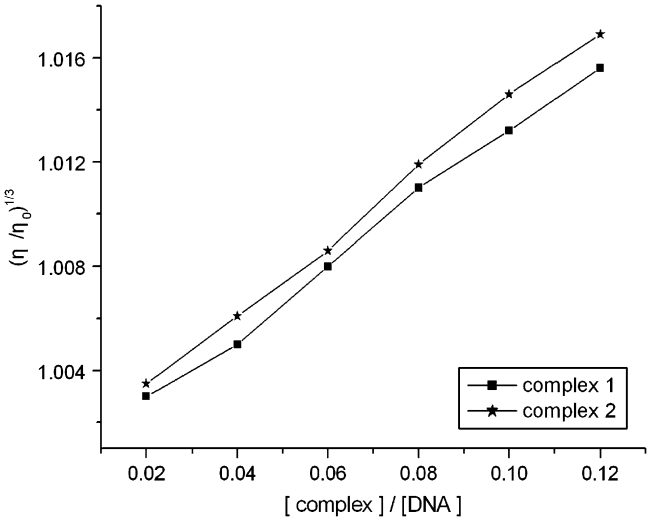

Fig. 8. Effect of increasing amounts of **1** and **2** on the relative viscosity of ct DNA at 25 °C. [DNA] = 50 μM, [complex] = 1, 2, 3, 4, 5, 6 μM.

Table 1
IC_{50} values for the cell growth inhibition.

Compound	IC_{50} value (μM)		
	GLC-82	ECA109	SGC7901
1	22.08	>50	19.98
2	16.20	21.04	15.40

measurements, we draw the conclusion that complexes **1** and **2** can bind to ct DNA in intercalative mode.

2.3. Pharmacology

2.3.1. Cytotoxic activities

Cytotoxicity of both complexes was investigated using MTT assay. Three different human cancer cell lines, lung adenocarcinoma (GLC-82) cell, esophagus squamous cancer (ECA109) cell and human gastric cancer (SGC7901) cell, were selected for the tests. The cell lines were treated with each complex at five grade concentrations for 48 h. (The results were afforded by the School of Pharmaceutical, Lanzhou University.) As shown in Figs. S1–S3 (see Supplementary data), both complexes exerted cytotoxic effect inhibiting the growth of all tested cell lines; the estimated IC_{50} are presented in Table 1. It is observed that both complexes show strong cytotoxic activities in vitro probably due to the complexes inducing DNA damage in cancer cells [14,15] and the features of the metal ions [42,43]. It is also observed that **2** shows more significant cytotoxic activities than **1** against the three human cancer cell lines, which is consistent with the results of DNA-binding studies.

2.3.2. Stability of the complexes in aqueous medium

The stability studies of the complexes were carried out by monitoring the electronic spectra of the complexes at 1×10^{-5} M in phosphate buffer (pH = 7.4) at 37 °C during 48 h. No obvious changes or isobestic point in electronic spectra was observed (shown in Figs. S4 and S5, see Supplementary data), also the color of the solution stayed colorless and clear over 48 h monitored, which illustrated that the complexes were stable under these conditions [44,45].

3. Conclusions

The two new complexes $ZnL_2 \cdot 2H_2O$ (**1**) and $CuL_2 \cdot 2H_2O$ (**2**) (HL = 1-hydroxy-6-(2-(1-piperidinyl)ethoxy)xanthone) have been synthesized and characterized. Their DNA-binding properties have been investigated by spectrophotometric methods and viscosity measurements. The results suggest that both the complexes can intercalate into the base pairs of DNA with strong binding affinities because of the good planarity of the xanthone ring. Furthermore, complex **2** shows stronger affinity than **1**. In addition, they have remarkable cytotoxic activities in vitro toward the GLC-82, ECA109 and SGC7901 cell lines. The present work may be helpful to the research of the anti-cancer mechanism of xanthones and the design of the new potent anti-cancer drugs.

4. Experimental

4.1. Chemistry

4.1.1. Materials and instruments

Isoeuxanthone (1,6-dihydroxyxanthone) and the ligand HL (1-hydroxy-6-(2-(1-piperidinyl)ethoxy)xanthone) were prepared according to the literature [16] with some improvement (shown in Fig. S6, see Supplementary data). 1-(2-Chloroethyl)piperidin hydrochloride was purchased from Alfa Aesar. The other chemicals were reagent grade and used without further purification.

Calf thymus DNA (ct DNA) and ethidium bromide (EB) were obtained from Sigma Chemical Co. All the measurements involving the interactions of the two complexes with ct DNA were carried out in doubly distilled water buffer containing 5 mM Tris and 50 mM NaCl, and adjusted to pH 7.1 with hydrochloric acid. UV–vis spectrometer was employed to check a solution of ct DNA purity (A_{260}:$A_{280} > 1.80$) and the concentration ($\varepsilon = 6600\ M^{-1}\ cm^{-1}$ at 260 nm) in the buffer [46,47].

Elemental analyses were conducted using an Elementar Vario EL elemental analyzer. The metal contents of the complexes were determined by titration with ethylenediaminetetraacetic acid (EDTA). Infrared spectra (4000–400 cm^{-1}) were performed on a satellite FTIR spectrometer (Thermo Mattson) with KBr as discs. ^1H NMR spectra were recorded using a Varian Mercury Plus 400 spectrometer. Conductivity measurements were performed in DMF with a DDS-11A conductor at room temperature. The UV–vis absorption spectra were recorded using a Varian Cary 100 spectrophotometer and fluorescence emission spectra were recorded using a Hitachi F-4500 spectrofluorophotometer.

4.1.2. DNA-binding measurements

Absorption and fluorescence titration experiments were performed at a constant concentration of the complexes (10 μM) while varying DNA concentration. The competitive binding experiments were carried out by maintaining the EB and ct DNA concentration at 2 μM and 30 μM, respectively, while increasing the concentrations of the complexes.

The CD spectra of DNA were recorded on a Jasco J-810 spectropolarimeter at 25.0 °C. The concentration of ct DNA used was 120 μM and the complexes solutions were added to a ratio of 3:1 (DNA/complex). Each sample solution was scanned in the range of 220–450 nm. CD spectrum represented the average of three scans with the buffer background subtracted.

Viscosity experiments were carried out on an Ubbelodhe viscometer, immersed in a thermostated water-bath maintained at 25.0 °C. Titrations were performed for the Zn(II) and Cu(II) complexes (1–6 μM), and each complex was introduced into DNA solution (50 μM) present in the viscometer. Flow time was measured with a digital stopwatch and each sample was measured three times and an average flow time was calculated. Data were presented as $(\eta/\eta_0)^{1/3}$ vs the ratio of the concentration of the complex to DNA, where η is the viscosity of DNA in the presence of complex, and η_0 is the viscosity of DNA alone. Viscosity values were calculated from the observed flow time of DNA-containing solution corrected from the flow time of buffer alone (t_0), $\eta = t - t_0$ [48,49].

4.1.3. Preparation of the complexes

*$ZnL_2{\cdot}2H_2O$ (**1**).* The ligand (HL) (135.6 mg, 0.4 mmol) was dissolved in 20 ml ethanol at 90 °C, and then solid NaOH (16 mg, 0.4 mmol) was added. After 0.5 h, $Zn(OAc)_2{\cdot}2H_2O$ (43.9 mg, 0.2 mmol) dissolved in 2 ml ethanol was added dropwise to the above solution. The mixture was refluxed, while stirring, for 8 h following which the yellow precipitate was collected, washed several times with ethanol–water (1:1) solution, dried in vacuo for 48 h. Yield: 106.2 mg (62%). Elemental Anal. Calcd for $C_{40}H_{44}N_2O_{10}Zn$: C, 61.74; H, 5.70; N, 3.60%. Found: C, 61.26; H, 5.60; N, 3.43%. IR ν_{max} (cm^{-1}): ν(–OH): 3427.2, ν(–CH_2–): 2960–2850, ν(–NCH_2–): 2803.5, ν(C═O): 1616.3, ν(C═C): 1455.1, ν(Ar–O): 1257.0, ν(C–O–C): 1178.2, ν(Ar–H): 767.0, ρ_w(O–H): 522.0, ν(M–O): 486.5. ^1H NMR (400 MHz, DMSO-d_6, 25 °C) δ (ppm): 8.04 (1H, d, Ar–H), 7.67 (1H, t, Ar–H), 7.16 (1H, dd, Ar–H), 7.07–7.04 (2H, m, Ar–H), 7.01 (1H, d, Ar–H), 4.23 (2H, t, –O–CH_2–), 2.67 (2H, t, –CH_2–N–), 2.47 (4H, t, –$N(CH_2)_2$–), 1.48–1.44 (4H, m, –CH_2–), 1.43–1.34 (2H, m, –CH_2–). Λ_M ($S\ cm^2\ mol^{-1}$): 5.4. λ_{max} (nm) (CH_3CH_2OH): 229, 302, 356.

*$CuL_2{\cdot}2H_2O$ (**2**).* The synthesis of **2** is identical to the synthesis of **1**. A yellow-green solid was collected. Yield: 125.6 mg (70%). Elemental Anal. Calcd for $C_{40}H_{44}N_2O_{10}Cu$: C, 61.88; H, 5.71; N, 3.61%; Found: C, 61.49; H, 5.8; N, 3.41%. IR ν_{max} (cm^{-1}): ν(–OH): 3419.9, ν(–CH_2–): 2960–2850, ν(–NCH_2–): 2803.0, ν(C═O): 1609.2, ν(C═C): 1458.0, ν(Ar–O): 1258.7, ν(C–O–C): 1184.5, ν(Ar–H) 769.6, ρ_w(O–H): 523.1, ν(M–O): 483.7 cm^{-1}. Λ_M ($S\ cm^2\ mol^{-1}$): 6.8. λ_{max} (nm) (CH_3CH_2OH): 229, 302, 356.

4.2. Pharmacology

4.2.1. Cell culture maintenance and drug solutions

Three different human cancer cell lines, lung adenocarcinoma (GLC-82), esophagus squamous cancer (ECA109) and human gastric cancer (SGC7901) cells were purchased from Shanghai Institutes for Biological Sciences, Chinese Academy of Sciences. The cytotoxicity assay was carried out in the three cell lines. Cells were cultured on RPMI-1640 medium supplemented with heat-inactivated fetal bovine serum (10%), penicillin (100 U/ml) and streptomycin (100 μg/ml) in 25 cm^2 culture flasks at 37 °C in a humidified atmosphere with 5% CO_2 and 95% air. In order to maintain the cells in log phase cellular suspension aliquots were refed with fresh RPMI-1640 medium two or three times per week.

Stock solutions of the two complexes were freshly prepared in DMSO and then diluted with the culture medium; less than 1% of DMSO was available at the final dilutions obtained.

4.2.2. Cytotoxic assay

The MTT assay was carried out as previously described [50] with minor modifications [51]. All cells to be tested in the following assays had a passage number of 3–6. For the drug treatment experiments, the cancer cells were harvested from the culture during the exponential growth phase and seeded into multiwell culture plates at 5×10^4 cells/ml in fresh medium. Following 24 h incubation at 37 °C, the cells were treated with the complexes at selected concentrations ranging from 4 to 64 μM for a period of 48 h. At the end of the drug treatment period, 10 μl of MTT solution (5 mg/ml) was added directly to all the appropriate wells and then the culture was incubated for 4 h. Thereafter the formazan crystal formed in the well was solubilized with DMSO and 100 μl of SDS (10%) was added to the system. After the plates were incubated overnight, the optical density was read on microplate spectrophotometer at 570 nm. Every test was run in triplicate. The relative inhibitory rate of cell growth by drugs was calculated by the formula: $R = (OD_{control} - OD_{test})/OD_{control} \times 100\%$, where R is the inhibitory rate of cell growth, OD_{test} is the absorbance value of cells in the presence of drugs and $OD_{control}$ is the absorbance value of control cells without any drug treatment.

4.2.3. Stability studies of the complexes

The two complexes were first dissolved in a minimum amount of DMSO (less than 1% of the final volume), and then diluted with phosphate buffer (pH 7.4). They were kept at 37 °C for 48 h. The stability studies were carried out by monitoring the electronic spectra of the resulting mixtures over 48 h.

Acknowledgement

We are grateful for the financial support of the National Science Foundation of China (20601011 and 20571035).

Appendix. Supplementary data

Supplementary data associated with this article can be found in the online version, at doi:10.1016/j.ejmech.2009.06.019.

References

[1] M.M.M. Pinto, M.E. Sousa, M.S. Nascimento, J. Curr. Med. Chem. 12 (2005) 2517–2538.
[2] V. Peres, T.J. Nagem, F.F.D. Oliveira, Phytochemistry 55 (2000) 683–710.
[3] H.A. Jung, B.N. Su, W.J. Keller, R.G. Mehta, A.D. Kinghorn, J. Agric. Food Chem. 54 (2006) 2077–2082.
[4] B.W. Lee, J.H. Lee, S.T. Lee, H.S. Lee, W.S. Lee, T.S. Jeong, K.H. Park, Bioorg. Med. Chem. Lett. 15 (2005) 5548–5552.
[5] M.V. Lembe'ge, S. Moreau, S. Larrouture, D. Montaudon, J. Robert, A. Nuhrich, Eur. J. Med. Chem. 43 (2008) 1336–1343.
[6] M. Pedro, F. Cerqueira, M.E. Sousa, M.S.J. Nascimento, M. Pinto, Bioorg. Med. Chem. 10 (2002) 3725–3730.
[7] P. Valenti, A. Bisi, A. Rampa, F. Belluti, S. Gobbi, A. Zampiron, M. Carrara, Bioorg. Med. Chem. 8 (2002) 239–246.
[8] N. Yoshimi, K. Matsunaga, M. Katayama, Y. Yamada, T. Kuno, Z. Qiao, A. Hara, J. Yamahara, H. Mori, Cancer Lett. 163 (2001) 163–170.
[9] K. Sanugul, T. Akao, Y. Li, N. Kakiuchi, N. Nakamura, M. Hattori, Biol. Pharm. Bull. 28 (2005) 1672–1678.
[10] E. Truscheit, W. Frommer, B. Junge, L. Muller, D.D. Schmidt, W. Wingender, Angew. Chem., Int. Ed.Engl. 20 (1981) 744–761.
[11] H. Madariaga, P.C. Lee, L.A. Heitlinger, M. Lenenthal, Dig. Dis. Sci. 33 (1988) 1020–1024.
[12] D.K. McCulloch, A.B. Kurtz, R.B. Tattersall, Diabetes Care 6 (1983) 483–487.
[13] S. Sou, H. Takahashi, R. Yamasaki, H. Kagechika, Y. Endo, Y. Hashimoto, Chem. Pharm. Bull. 49 (2001) 791–793.
[14] G. Zuber, J.C.J. Quada, S.M. Hecht, J. Am. Chem. Soc. 120 (1998) 9368–9369.
[15] V.S. Li, D. Choi, Z. Wang, L.S. Jimenez, M.S. Tang, H. Kohn, J. Am. Chem. Soc. 118 (1996) 2326–2331.
[16] Y. Liu, L. Zou, L. Ma, W.H. Chen, B. Wang, Z.L. Xu, Bioorg. Med. Chem. 14 (2006) 5683–5690.
[17] S. Woo, J. Jung, C. Lee, Y. Kwon, Y. Na, Bioorg. Med. Chem. Lett. 17 (2007) 1163–1166.
[18] N. Fonteneau, P. Martin, M. Mondon, H. Ficheux, J.P. Gesson, Tetrahedron 57 (2001) 9131–9135.
[19] R.A. Dodean, J.X. Kelly, D. Peyton, G.L. Gard, M.K. Riscoe, R.W. Winter, Bioorg. Med. Chem. 16 (2008) 1174–1183.
[20] W.J. Geary, Coord. Chem. Rev. 7 (1971) 81–122.
[21] Infrared and Raman Spectra of Inorganic and Coordination Compounds, fourth ed. John Wiley & Sons, 1986, p. 257.
[22] M. Peters, L. Siegfried, T.A. Kaden, J. Chem. Soc., Dalton Trans. (2000) 4664–4668.
[23] M.H.V. Werts, J.W. Verhoeven, J.W. Hofstraat, J. Chem. Soc., Perkin Trans. 2 (2000) 433–439.
[24] J.M. Kelly, M.J. Murphy, D.J. Mcconnell, C. Ohuigin, Nucleic Acids Res. 13 (1985) 167–184.
[25] V.A. Bloomfield, D.M. Crothers, I.J.I. Tinico, Physical Chemistry of Nucleic Acids, Harper and Row, New York, 1974.
[26] A. Wolf, G.H. Shimer Jr., T. Meehan, Biochemistry 26 (1987) 6392–6396.
[27] S. Satyanarayana, J.C. Dabrowiak, J.B. Chaires, Biochemistry 31 (1992) 9319–9324.
[28] S.J. Lippard, Acc. Chem. Res. 11 (1978) 211–217.
[29] J.B. Lepecq, C. Paoletti, J. Mol. Biol. 27 (1967) 81–90.
[30] Y.B. Zeng, N. Yang, W.S. Liu, N. Tang, J. Inorg. Biochem. 97 (2003) 258–264.
[31] C.V. Kumar, J.K. Barton, N.J. Turro, J. Am. Chem. Soc. 107 (1985) 5518–5582.
[32] M.R. Efink, C.A. Ghiron, Anal. Biochem. 114 (1981) 199–206.
[33] T.R. Li, Z.Y. Yang, B.D. Wang, D.D. Qin, Eur. J. Med. Chem. 42 (2007) 1–8.
[34] V.I. Ivanov, L.E. Minchenkova, A.K. Schyolkina, A.I. Poletayer, Biopolymers 12 (1973) 89–110.
[35] P. Lincoln, E. Tuite, B. Norden, J. Am. Chem. Soc. 119 (1997) 1454–1455.
[36] B. Norden, F. Tjerneld, Biopolymers 21 (1982) 1713–1734.
[37] V.G. Vaidyanathan, R. Vijayalakshmi, V. Subramanain, B.U. Nair, Bull. Chem. Soc. Jpn. 75 (2002) 1143–1149.
[38] M. Chauhan, F. Arjmand, Chem. Biodiv. 3 (2006) 660–676.
[39] P. Uma Maheswari, M. Palaniandavar, J. Inorg. Biochem. 98 (2004) 219–230.
[40] B.I. Kankia, V. Buckin, V.A. Bloomfield, Nucleic Acids Res. 29 (2001) 2795–2801.
[41] X.H. Zou, B.H. Ye, H. Li, J.G. Liu, Y. Xiong, L.N. Ji, J. Chem. Soc., Dalton Trans. (1999) 1423–1428.
[42] M. Viola-Rhenals, M.S. Rieber, M. Rieber, Biochem. Pharmacol. 71 (2006) 722–734.
[43] K.G. Daniela, P. Guptaa, R.H. Harbachb, W.C. Guidab, Q.P. Dou, Biochem. Pharmacol. 67 (2004) 1139–1151.
[44] E. Cabrera, H. Cerecetto, M. González, D. Gambino, P. Noblia, L. Otero, B. Parajón-Costa, A. Anzellotti, R. Sánchez-Delgado, A. Azqueta, A.L. de Ceráin, A. Monge, Eur. J. Med. Chem. 39 (2004) 377–382.
[45] C.P. Tan, J. Liu, L.M. Chen, S. Shi, L.N. Ji, J. Inorg. Biochem. 102 (2008) 1644–1653.
[46] T.C. Michael, R. Marisol, J.B. Allen, J. Am. Chem. Soc. 111 (1989) 8901–8911.
[47] C.V. Kumar, E.H. Asuncion, J. Am. Chem. Soc. 115 (1993) 8547–8553.
[48] M. Eriksson, M. Leijon, C. Hiort, B. Norden, A. Gradslund, Biochemistry 33 (1994) 5031–5040.
[49] Y. Xiong, X.F. He, X.H. Zou, J.Z. Wu, X.M. Chen, L.N. Ji, R.H. Li, J.Y. Zhou, K.B. Yu, J. Chem. Soc., Dalton Trans. (1999) 19–23.
[50] T. Mosmann, J. Immunol. Methods 65 (1983) 55–63.
[51] S.M. Konstantinov, H. Eibl, M.R. Berger, Br. J. Haematol. 107 (1999) 365–374.